



Exploring DNA barcode for accurate identification of threatened *Aconitum* L. species from Western Himalaya

Anita Choudhary^{1,2} · Deepika Shekhawat¹ · Jyotsna Pathania¹ · Kumari Sita³ · Shailika Sharma³ · Amit Chawla^{2,3} · Vandana Jaiswal^{1,2}

Received: 22 August 2023 / Accepted: 27 November 2023
© The Author(s), under exclusive licence to Springer Nature B.V. 2023

Abstract

Background *Aconitum* species, belonging to Ranunculaceae, have high medicinal importance but due to their overexploitation come under IUCN (International Union for Conservation of Nature) red list. The precise identification of the *Aconitum* species is equally important because they are used in herbal formulations. The present study aimed to develop an efficient DNA barcode system for the authentic identification of *Aconitum* species.

Methods and results A set of 92 barcode gene sequences (including 12 developed during the present study and 80 retrieved from NCBI) of 5 *Aconitum* species (*A. heterophyllum*, *A. vialoceanum*, *A. japonicum*, *A. napellus*, and *A. stapfianum*) were analyzed using three methods (tree-based, distance-based, and similarity-based) for species discrimination. The PWG-distance method was found most effective for species discrimination. The discrimination rate of PWG-distance ranged from 33.3% (rbcL+trnH-psbA) to 100% (ITS, rbcL+ITS, ITS+trnH-psbA and rbcL+ITS+trnH-psbA). Among DNA barcodes and their combinations, the ITS marker had the highest degree of species discrimination (NJ-40%, PWG-100% and BLAST-40%), followed by trnH-psbA (NJ-20%, PWG-60% and BLAST-20%). ITS also had higher barcoding gap as compared to other individual barcodes and their combinations. Further, we also analyzed six *Aconitum* species (*A. balfourii*, *A. ferox*, *A. heterophyllum*, *A. rotundifolium*, *A. soongaricum* and *A. violaceum*) existing in Western Himalaya. These species were distinguished clearly through tree-based method using the ITS barcode gene with 100% species resolution.

Conclusion ITS showed the best species discrimination power and was used to develop species-specific barcodes for *Aconitum* species. DNA barcodes developed during the present study can be used to identify *Aconitum* species.

Keywords DNA barcoding · Species discrimination · Interspecific distance · Phylogenetic tree

Abbreviation

BLAST	Basic Local Alignment Search Tool	CO1	Flora
CBOL	Consortium for the Barcode of Life	CP	Cytochrome c oxidase 1
CITES	Convention on International Trade in Endangered Species of Wild Fauna and	CTAB	Chloroplast
		EN	Cetyl Trimethyl Ammonium Bromide
		IUCN	Endangered
			International Union for Conservation of Nature
		K2P	Kimura-2-parameter
		matK	maturase-K
		NCBI	National Center for Biotechnology Information
		nrITS	nuclear ribosomal Internal Transcribed Spacer
		PWG-distance	Pairwise-Genetic Distance
		rbcL	ribulose-bisphosphate/carboxylase Large-subunit gene
		SCAR	Sequence Characterized Amplified

✉ Vandana Jaiswal
vandana.jaiswal2009@gmail.com; vandana@ihbt.res.in

¹ Biotechnology, Division, CSIR-Institute of Himalayan Bioresource Technology, Palampur, Himachal Pradesh 176061, India

² Academy of Scientific and Innovative Research (AcSIR), Ghaziabad 201002, India

³ Environmental Technology Division, CSIR-Institute of Himalayan Bioresource Technology, Palampur, Himachal Pradesh 176061, India

	Region
SNPs	Single Nucleotide Polymorphisms
VU	Vulnerable

Introduction

The correct identification and distinction of different plant species are challenged by the vegetative characteristics when they are quite similar to one another and reproductive parts are not available. This is especially required in the case of medicinal plants; whose authenticity needs to be determined before these are utilized for important formulations. Additionally, other challenges that put off the safety and herbal efficacy of medicinal plants are the inability to accurately separate them from their similar relatives, adulterants, and counterfeits [1]. Further, medicinal plants have an ever-growing market for herbal-based drugs, and uncontrolled harvesting has resulted in many of them becoming rare or threatened. The Himalayan range is a storehouse of plant biodiversity with more than 8,000 species reported in the eco-region, of which about 1748 species have been said to possess medicinal properties [2]. In this eco-region, medicinal plants are continuously exploited due to the demand by pharmaceutical companies, and being harvested from the wild in large quantities. This has resulted in most of these plant species being listed in IUCN (International Union for Conservation of Nature) red list and many of them finding place in different Appendices of CITES (Convention on International Trade in Endangered Species of Wild Fauna and Flora), prohibiting their trade. However, their trade keeps continuing due to demands, although not through legalized channels. Further, there is a probability that the traded material is not of the actual species but adulterated with other species with similar morphological characteristics of traded part(s). The inability to identify them either as a collected specimen or in fragmented form (plant parts as medicines) makes it challenging to enforce the prohibitions placed on their unsustainable harvesting and illegal trafficking. At times the identity is also faked with other plant species which are legalized for trade to avoid detection of prohibited plant species. Thus, there are a large number of plants which are extracted from the Himalaya which have become threatened in recent years due to unsustainable harvesting. Lack of organized cultivation and indiscriminate harvesting has caused the wild germplasm of these species to be depleted. Hence, conservation efforts are also required for the correct identification of medicinal plant species, as a first step. Therefore, there is a significant need for biotechnology-based interventions such as DNA barcoding, in order to ensure true identification of these species and their conservation. Each barcode exhibits a distinct genetic

variation which is specific to each species and is able to differentiate between closely related species. Thus, DNA barcoding techniques have proved a promising approach for identifying plant species, and databases of DNA sequences of the nuclear or organelle genome of different plant species are now readily available and continuously being updated [3].

In DNA barcoding, short, varied, and uniform DNA sections are used to identify and distinguish between different species [4–6]. It was introduced as a revolutionary method for rapid and extensive species identification employing unique gene sequences as molecular species-specific marks two decades ago [4]. Three fundamental requirements must be fulfilled for a DNA sequence to be useful as a barcode: (i) significant genetic variation at the species level to allow species discrimination, (ii) a short sequence length to support DNA extraction and amplification, and (iii) primer universality across highly divergent taxa [5, 7, 8]. It was initially proposed in animals and extensively used [4]. The cytochrome c oxidase 1 (CO1), which has been proven to be universally relevant in animal barcoding, is not acceptable for most species of plants because of a substantially slower rate of cytochrome c oxidase 1 gene mutation in higher plants than in animals [5, 9]. All of the existing loci do not operate across all species, despite the fact that numerous researchers have looked for a universal plant barcode [10, 11]. The matK and rbcL two-locus combination has been selected as the best plant barcode by the Consortium for the Barcode of Life-Plant Working Group (CBOL) [12, 13] while other researchers proposed that differentiating between plant species may need the use of a multi-locus technique. There are four standard barcodes which are being utilized as the core barcode markers for the molecular identification of plants: the ribulose-bisphosphate/carboxylase Large-subunit gene (rbcL), the maturase-K gene (matK), the trnH-psbA intergenic spacer, and the nuclear ribosomal internal transcribed spacers (nrITS) [14–17]. Combining plastid (matK, rbcL, and psbA-trnH) and nuclear (ITS) regions has been suggested as a potential way to categorise different plant species.

Aconitum, a member of the Ranunculaceae family, contains about 350 species, are found primarily in Asia, accompanied by Europe and North America. Many species of *Aconitum* plants were employed in traditional medicine, primarily have the properties analgesic, anti-inflammatory, antirheumatic, and cardiotoxic while some are poisonous [18]. Due to their exploitation for high medicinal uses, the *Aconitum* species, under the present study, are included in the IUCN Red List [19–21], with *A. heterophyllum* and *A. violaceum* categorized as ‘Endangered’ and ‘Vulnerable’ respectively. Microsatellite markers were used to study genetic diversity and population structure in order to gain

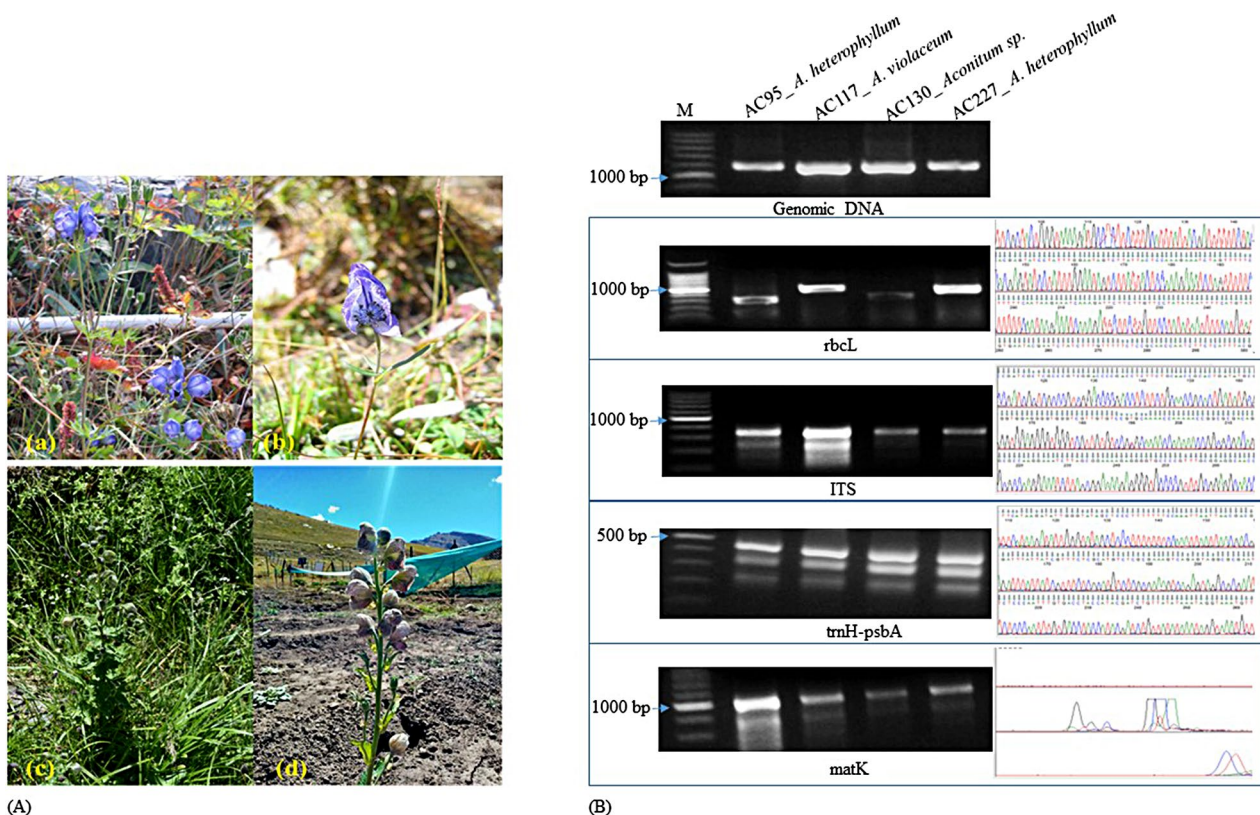


Fig. 1 Representative images showing (A) flowering stage of *Aconitum heterophyllum* (a, b) and *A. violaceum* (c,d) in their natural habitat of Western Himalaya (B) intact genomic DNA and successful amplification of four DNA barcodes in *Aconitum* samples collected during the present study. The expected product size of rbcL = 554 bp, ITS = 707 bp, trnH-psbA = 450 bp, and matK = 900 bp. In case of rbcL, different sizes of bands are amplified in different samples suggested

that the sequence variations among the samples, but the variation is not species-specific. In other barcode genes like ITS, trnH-psbA and matK, some non-specific bands also amplified, but sequencing was done for specific bands after purification. The sequencing was successfully done in the case on rbcL, ITS and trnH-psbA, however, in case of matK, sequencing failed

access to its conservation and population status [22]. Further, the precise identification of these *Aconitum* species is equally important particularly if they are used in herbal formulations. Some efforts have been made in the development of DNA barcode of *Aconitum* for species identification, but with a limited number of species, and only single barcode gene was explored (psbA-trnH [23], ITS2 [24], ITS and matK [25], and rbcL [26]).

The present study focused to develop efficient DNA barcodes for species identification of *Aconitum*, with particular emphasis on the species of Western Himalaya. Fresh samples of *Aconitum* species were collected from Western Himalaya. Four DNA barcodes were explored in all the *Aconitum* species (including those collected during the present study, and all available sequences on databases). The present study investigated the effectiveness of individual barcodes and their combination for species differentiation; and develop an efficient barcode system to identify *Aconitum* species.

Table 1 Summary of total sequences and aligned length of individual barcodes and their combinations used during the present study

DNA barcode region	No. of individual sequences (species)	Sequence length (bp)	Aligned length (bp)
rbcL	45 (5)	307–1480	124
ITS	39 (5)	361–749	450
trnH-psbA	8 (5)	222–411	157
rbcL + ITS	13 (4)	574	452
rbcL + trnH-psbA	6 (3)	281	258
ITS + trnH-psbA	6 (3)	607	595
rbcL + ITS + trnH-psbA	6 (3)	731	706

Materials and methods

Sampling site and sample collection of *Aconitum* spp

Multiple accessions were collected from the wild for *A. heterophyllum* (Trade name: Patish; IUCN Red List:

Endangered (EN)) and *A. violaceum* (trade name: Mitha Patish; IUCN Red List: Vulnerable (VU)) from Himachal Pradesh State of India. This area forms a part of the Western Himalayan region, which is the native distributional range of these species. Both the species have patchy distribution in alpine areas of this eco-region and are included in various IUCN red list threat categories, as per 'global assessment'. Although there are other species such as *A. balfourii*, *A. ferox*, *A. rotundifolium*, *A. soongaricum*, *A. deinorhizum*, *A. chasmanthum* etc., but as these are much rare to find in Himachal Pradesh, and thus, were not included in the present study. Further, the 02 species under consideration have been reported to be under severe threat [27] due to rampant extractions in the region and are reported to be highly traded in recent years [28, 29]. Voucher specimens of these species were collected and deposited in CSIR-IHBT's herbarium, and identified to the species level using local floras and existing specimens.

DNA extraction, PCR amplification and sequencing of collected samples

For DNA extraction, fresh leaves of above-mentioned plant samples were collected in silica gel. High quality genomic DNA were extracted using cetyltrimethylammonium bromide (CTAB) method [30]. Quality and quantity of extracted DNA were checked using 1.0% agarose gel and nanodrop (Thermo Fisher, NanoDrop™ One/OneC micro-volume), respectively. The extracted DNA was diluted with nucleus free water to a final concentration of 50 ng/μl for PCR amplification with four most widely used plant DNA barcodes. These barcodes included *rbcL*, *ITS*, *trnH-psbA* and *matK*; details are provided in Table S1. For each DNA barcode, PCR was performed in final volume 20 μl with following reaction composition- 2 μl of template DNA, 4 μl of 5x Colourless Go Taq® Flexi Buffer, 2 μl of 25mM MgCl₂, 0.4 μl dNTPs, 0.1 μl Taq DNA polymerase, 1 μl of each primer (forward and reverse). The amplification was done with following thermal profile- 94°C for 4 min, 36 cycles of 94°C for 30 s, 48–55°C for 30 s, and 72°C for 1 min followed by a final extension at 72°C for 5 min using C1000 Touch™ Thermal Cycler (Bio-Rad). The amplified products were resolved on 1.5% agarose gel to examine the single amplicon.

In cases, where multiple bands were amplified, the desired product was eluted from the gel using MinElute® Gel Extraction Kit (Qiagen) following manufacturer's protocol. The eluted product was re-amplified with corresponding primers to get the single amplicon. The PCR products were cleaned up with ExoSAP-IT™ (Applied Biosystems) following the manufacturer's protocol and sequenced using ABI 3130xl DNA Analyzer (Applied Biosystems).

Sequencing was done in both directions (forward and reverse primers) using BigDye™ Terminator v3.1 Cycle Sequencing Kit (Applied Biosystems).

Sequence retrieval of DNA barcode of *Aconitum* Sp from NCBI

In order to develop the efficient DNA barcode, all the DNA barcode sequence of *Aconitum* sp available on National Center for Biotechnology Information (<https://www.ncbi.nlm.nih.gov/>) was also searched and retrieved. (Table S2). We excluded the species, where only single sequence of DNA barcode was available due to statistical reasons.

Sequence alignment and nucleotide diversity

The raw sequences were checked for their quality using software FinchTV version 1.4.0 and only high-quality sequences were utilized for downstream analysis. All the sequences (including both, retrieved from NCBI and generated during the present study) of individual barcodes were aligned using MUSCLE in MEGA X software [31] and unaligned nucleotides from both the ends were trimmed manually. Nucleotide base frequency in protein-coding region, candidate nucleotide at particular codon position and nucleotide pair frequency were also calculated for individual barcode and their combinations using MEGA X software. The aligned sequences were analyzed for different parameters of nucleotide variation like number of variable sites, number of informative sites, and number of segregating sites using DnaSP v6.12.03 software [32]. Nucleotide diversity and neutrality tests were performed to assess the genetic diversity. The possibility of recent population growth was examined through two statistical tests- Tajima's D [33] and Fu's Fs [34] using DnaSP v6.12.03 software. The populations' mismatch frequency graphs were produced under a constant population size model to see if they showed signs of a stable population history [33].

Species discrimination

In the present study, three commonly used methods; tree-based, distance-based, and similarity-based (BLAST-Basic Local Alignment Search Tool) were applied to the individual DNA barcode and their potential combinations to assess the effectiveness of species discrimination.

Tree-based approach

In this approach, discrimination effectiveness of individual barcodes or their combinations is determined based on the proportion of monophyletic species in dendrograms.

Unrooted neighbour-joining (NJ) trees were built using p-distance and pairwise deletion model for the tree-based technique in MEGA X [35–37]. Node support was determined using 1000 bootstrap replicates. Species discrimination was considered successful when every individual of the same species belonged to a single clade [7]. The species discrimination rate for a DNA barcode region was calculated as the number of species which did not cluster with individuals of any other species divided by the total number of species used.

Distance-based approach

In this approach, pairwise-genetic distance (PWG-distance) was calculated using Kimura-2-parameter (K2P) model using MEGA X software. Inter- and intra-specific genetic distances were used to calculate barcoding gaps [7, 38]. No species discrimination was considered when the interspecific genetic distance between the corresponding species was estimated as zero (0.0) [39]. Species discrimination rate was calculated as the number of species having K2P distance zero with any other species divided by the total number of species that have been analyzed for a DNA barcode region.

Similarity-based approach

In this approach, NCBI BLAST program was used and all sequences were queried using the blastn command. Discrimination of a species was considered satisfactory if all the members of a species appeared in top matching hit. If all the sequences of a species showed 100% match (query cover and percent identity) or maximum with only same species, not with others, then species identification was considered successful. The species discrimination rate was calculated as the number of species which matched with same species divided by the total number of species used.

Results

Morphological features of *Aconitum* spp

The plants of *A. heterophyllum* are erect, herbaceous perennials, and their height varies from 30 to 100 cm with ovoid or fusiform roots. Stem is simple or sometimes branches arose from the lower part, glabrous with a few very short crispate hairs above. Lower leaves are long petiolate, usually 5 lobed and orbicular-cordate to ovate-cordate in shape. Upper leaves are short petiolate or sessile, lanceolate and irregularly crenate-dentate. Inflorescence is loose raceme, greenish blue in colour with dark purple veins (Fig. 1A).

Table 2 Nucleotide pair frequencies of individual nucleotide sequences of three barcodes and their combinations used during the present study

DNA barcode	ii						sv						R											
	Avg		1st		2nd		3rd		Avg		1st		2nd		3rd		Avg		1st		2nd		3rd	
rbcL	106	35	36	35	2	1	0	1	1	2	1	0	1	1.1	1.3	0.8	1.0							
ITS	440	146	146	147	3	1	1	1	4	4	1	2	1	0.9	1.2	0.6	1.2							
trnH-psbA	106	37	34	35	11	4	4	4	11	3	3	4	3	1.0	1.3	0.9	1.1							
rbcL + ITS	439	147	147	146	6	2	2	2	4	4	0	2	2	1.4	6.6	0.8	1.1							
rbcL + trnH-psbA	222	76	71	75	13	3	5	5	14	4	4	6	4	0.9	0.8	0.9	1.1							
ITS + trnH-psbA	551	187	184	180	18	5	6	6	16	5	5	5	6	1.1	1.0	1.1	1.3							
rbcL + ITS + trnH-psbA	657	223	220	215	20	5	6	6	19	6	6	6	7	1.1	0.8	1.0	1.4							

ii = Identical pairs; si = Transitional pairs; sv = Transversional pairs; R = si/sv

Sepals are petaloid, blue to violet, glabrous and erect; the upper sepals are helmet shape and the lateral sepals are narrow.

A. violaceum is perennial, erect or ascending herbaceous plant, height upto 30 cm. Stem is usually simple, erect in the lower part and rarely branched, glabrous or hairy. Lower leaves are long-petioled, forming cluster near the base, deeply penta-partite towards the base; lobes are further divided into linear segments. Upper leaves are small in size, shortly petioled or sessile. Flowers are large in size, violet to bluish-purple in colour and arranged in corymbs or short racemes (Fig. 1A).

PCR amplification and sequencing success rate

High-quality genomic DNA was extracted from all the collected samples and successfully amplified with all four DNA barcodes including *rbcL*, ITS, *trnH-psbA* and *matK*. Sequencing was successful with three DNA barcodes i.e. *rbcL*, ITS, *trnH-psbA* (Supplementary dataset S1). However, in case of *matK*, sequencing failed repeatedly (Fig. 1B), and thus *matK* barcode was excluded from downstream analysis.

Sequence retrieval from NCBI

On NCBI database, DNA barcodes were available for total 193 *Aconitum* species (Table S3). However, out of 193 species, DNA sequences of all the three barcodes (i.e. *rbcL*, ITS and *trnH-psbA*) were available for only three species (*A. japonicum*, *A. napellus*, and *A. stapfianum*); and thus included in downstream analysis during the present study. For remaining (190) species, sequences were available for only one or two barcodes.

A total 80 barcode sequences were retrieved from NCBI representing five *Aconitum* species (Table S2). These species included two species (*A. heterophyllum* and *A. violaceum*) for which sampling has been done from Western Himalaya during the present study; and three species (*A. japonicum*, *A. napellus*, *A. stapfianum*) for which all the DNA barcodes were available on the NCBI. For individual barcode, maximum 41 sequences were retrieved for *rbcL*, followed by 35 sequences for ITS, and minimum of four (4) sequences for *trnH-psbA*.

Sequence characteristics

A total 92 sequences (including 12 developed during the present study and 80 retrieved from NCBI) of 5 *Aconitum* species were used for the development of efficient DNA barcodes for species discrimination during present study. For individual barcode and their combinations, length of

aligned sequences varied from 124 bases (*rbcL*) to 706 bases (*rbcL*+ITS+*trnH-psbA*), Table 1. For *rbcL*, total 45 sequences (length 307–1480 bases) were used for alignment, and 124 bases long aligned sequences were obtained. Similarly, for ITS and *trnH-psbA*, total 39 (length 361–749 bases) and eight (8) (length 222–411 bases) sequences were aligned, respectively. In case of ITS, final aligned sequence was 450 bases and for *trnH-psbA*, the final aligned sequence was 157 bases long.

Nucleotide frequency and average AT and GC content at various codon coding sites are given in Table S4. Frequencies of individual nucleotides were found variable for different barcodes and their combinations. For instance, in case of *rbcL*, the maximum frequency was observed for thymine (T, 36.7%) followed by adenine (A, 28.0%); similar was the case for *trnH-psbA* where T and A represented 40.5% and 26.7%, respectively. However, in case of ITS, the maximum proportion was covered by cytosine (C) and guanine (G).

As per the individual position of codon (1st, 2nd, and 3rd) is concerned, maximum difference in the proportion of AT and CG contents was observed at 3rd position of the codon in majority of barcodes as well as their combinations; although, the differences in the proportion found variable in different barcodes and their combinations (Table S4). For instance, in case of *rbcL*, AT content was found higher (78.1%) at third position of codon as compared to the GC content (21.9%); however, opposite was observed for ITS where GC content was higher (61.9%) at third position of codon as compared to the AT content (38.2%).

Nucleotide pair frequency suggested that most of the nucleotide pairs were identical as expected; and few mutation events were also observed in each barcode (Table 2). Maximum 22 mutations (11 each transition and transversion) were observed in *trnH-psbA*, followed by seven (7) mutations in ITS and four (4) mutations in *rbcL*. Transition/transversion ratio slightly varied across the individual barcode and ranged 0.9 (ITS) to 1.1 (*rbcL*). In case of barcode combinations, nucleotide pair frequencies including identical pairs, transition and transversion events varied proportionally (Table 2).

Genetic diversity

Aligned sequences of individual barcodes and their combinations were analysed for different variability parameters (Table 3). As expected, maximum variable sites (102) and maximum informative sites (25), were observed in case of barcode combination *rbcL*+ITS+*trnH-psbA*. However, maximum proportion of variable sites (39.49%) and informative sites (5.73%) were observed in *trnH-psbA*. ITS showed minimum proportion (less than 10%) of indel events; however, other two DNA barcodes showed that all

Table 3 Nucleotide variation of DNA barcodes and their combinations used in the present study

DNA barcode region	No. of variable sites	No. of informative sites	No. of indel events
rbcL	45 (36.29)	7 (5.64)	45
ITS	51 (11.33)	21 (4.67)	5
trnH-psbA	62 (39.49)	9 (5.73)	61
rbcL+ITS	29 (6.41)	17 (3.76)	5
rbcL+trnH-psbA	75 (29.06)	11 (4.26)	15
ITS+trnH-psbA	92 (15.46)	15 (2.52)	16
rbcL+ITS+trnH-psbA	102 (14.44)	25 (3.54)	16

* values given in parentheses are per cent values

the variability arose due to indels, except one variable event in case of trnH-psbA.

Different parameters of nucleotide diversity and neutrality tests for each DNA barcodes and their combinations are shown in Table 4. The maximum average number of nucleotide difference between pairs of sequences were observed in barcode combination rbcL+ITS+trnH-psbA (39.533) as expected. Among individual barcodes, maximum average number of nucleotide differences between pairs of sequences were observed in trnH-psbA (17.75) and lowest in rbcL (3.002). On the basis of Eta value, rbcL+ITS+trnH-psbA showed highest nucleotide diversity (102) and rbcL showed the lowest (47) among all DNA barcodes and combinations. Total number of mutations (Eta) varied 29 (rbcL+ITS) to 102 (rbcL+ITS+trnH-psbA). Haplotype diversity (Hd) ranged from 0.245 (rbcL) to 1.0 (ITS+trnH-psbA and rbcL+ITS+trnH-psbA). Further, rbcL+ITS had minimum (0.0209) nucleotide substitution rate and ITS showed minimum nucleotide diversity (0.01596); however, maximum nucleotide substitution rate (0.26113) and nucleotide diversity (0.18490) was found in case of trnH-psbA.

Fu's Fs neutrality test revealed that only ITS marker had a negative value (-0.494). Tajima's D values for all markers were negative except rbcL+ITS (0.17466) but statistically non-significant (Table 4), indicating a greater number of

unusual nucleotide site variations that would be expected by a neutral model of evolution. The nucleotide mismatch distribution analysis was done among various sequences (Fig. S1). DNA sequences were evaluated for population size changes, which expanded the findings of genetic diversity among species. All the sequences showed genetic variations.

Species discrimination using different methods

Three techniques (NJ, PWG-Distance, and Blast) were used to assess the effectiveness of species discrimination for DNA barcodes and combinations.

Tree based

The effectiveness of identification at the species levels was evaluated using the NJ approach. Successful species identification was considered to have occurred when members of a species formed a monophyletic clade or were close to each other (Fig. 2). The marker combinations rbcL+ITS, ITS+trnH-psbA, and rbcL+ITS+trnH-psbA all demonstrated species discrimination, with the exception of rbcL+trnH-psbA. All individuals in the NJ tree of ITS, cluster together across all areas, demonstrating the best species discrimination (Fig. 2).

Distance-based

The highest pairwise genetic distance (overall mean) observed 28.97% (trnH-psbA) followed by 13.73% (rbcL+trnH-psbA), and 6.35% (ITS+trnH-psbA) whereas lowest 1.59% (ITS) accompanied by 2.21% (rbcL+ITS), 5.62% (rbcL), and 6.09% (rbcL+ITS+trnH-psbA). The intra- and inter-specific genetic distance with each barcode and their combinations for each species are depicted in Table 5. Among all the barcodes and their combination, ITS performed better in order to discriminate the species. In ITS, intraspecific genetic distance was found lower than the

Table 4 Genetic diversity of individual barcodes and their combinations and Fu's F and Tajima's D test (neutrality tests)

DNA Barcode	n	Nucleotide diversity			θ	π	Neutrality tests			
		k	Eta	Hd			Fu's Fs	p-value	D	p-value
rbcL	45	3.00	47	0.245	0.13606	0.03800	5.161	0.998	-2.515	<0.001
ITS	39	7.10	51	0.889	0.02711	0.01596	-0.494	0.835	-1.47137	>0.10
trnH-psbA	8	17.75	65	0.643	0.26113	0.18490	6.234	0.997	-1.57903	0.10 > p > 0.05
rbcL+ITS	13	9.72	29	0.936	0.02091	0.02174	0.720	0.743	0.17466	>0.10
rbcL+trnH-psbA	6	27.20	75	0.733	0.13517	0.11193	8.101	1.000	-1.10786	>0.10
ITS+trnH-psbA	6	34.20	92	1.000	0.06959	0.05907	0.660	0.739	-0.97647	>0.10
rbcL+ITS+trnH-psbA	6	39.53	102	1.000	0.06474	0.05729	0.827	0.696	-0.74354	>0.10

n = Number of nucleotide sequences; k = Average number of nucleotide difference between pairs of sequences; Eta = Total number of mutations; Hd = Haplotype (gene) diversity; θ = Nucleotide substitution rate; π = Nucleotide diversity; Fu's Fs = variation among different haplotypes in the population; D = Tajima test statistic

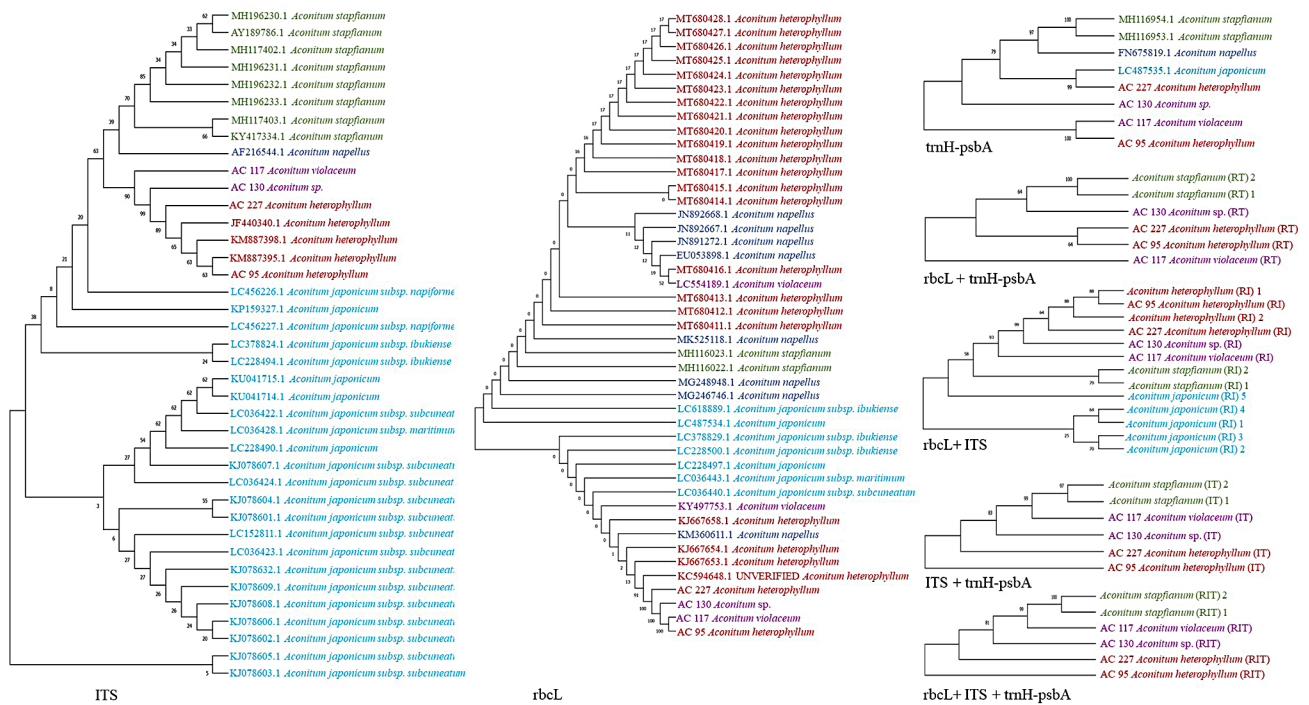


Fig. 2 The neighbor-joining (NJ) tree constructed for *Aconitum* species under p-distance model using DNA barcode markers using different DNA barcode genes and their available combinations. ITS showed the best discrimination between the *Aconitum* species among all the bar-

code genes/combinations. rbcL and trnH-sbA do not discriminate the *Aconitum* species individually, but species discrimination is enhanced for these barcodes while used in combination with ITS.

Table 5 Comparison of the genetic distances at three different loci and their possible combinations under K2P distance between and within five different species of *Aconitum*

Species	1	2	3	4	5	6	7
Intraspecific Mean Distance							
<i>Aconitum heterophyllum</i>	0.0931	0.0140	0.5482	0.0054	0.2189	0.0863	0.0714
<i>Aconitum japonicum</i>	0.0000	0.0021	n/c	0.0022	-	-	-
<i>Aconitum napellus</i>	0.0000	n/c	n/c	-	-	-	-
<i>Aconitum stapfianum</i>	0.0000	0.0029	0.0000	0.0044	0.0000	0.0034	0.0029
<i>Aconitum violaceum</i>	0.0731	n/c	n/c	n/c	n/c	-	n/c
Interspecific Mean Distance							
<i>A. heterophyllum</i> and <i>A. stapfianum</i>	0.0477	0.0417	0.2861	0.0352	0.1642	0.0695	0.0733
<i>A. heterophyllum</i> and <i>A. japonicum</i>	0.0477	0.0370	0.5820	0.0319	-	-	-
<i>A. heterophyllum</i> and <i>A. violaceum</i>	0.0744	0.0455	0.2741	0.0410	0.1094	0.0726	0.0601
<i>A. heterophyllum</i> and <i>A. napellus</i>	0.0477	0.0496	0.3171	-	-	-	-
<i>A. stapfianum</i> and <i>A. japonicum</i>	0.0000	0.0089	0.2875	0.0080	-	-	-
<i>A. stapfianum</i> and <i>A. violaceum</i>	0.0320	0.0345	0.0071	0.0342	0.0449	0.0276	0.0381
<i>A. stapfianum</i> and <i>A. napellus</i>	0.0000	0.0244	0.0309	-	-	-	-
<i>A. japonicum</i> and <i>A. violaceum</i>	0.0320	0.0291	0.2875	0.0287	-	-	-
<i>A. japonicum</i> and <i>A. napellus</i>	0.0000	0.0198	0.2615	-	-	-	-
<i>A. napellus</i> and <i>A. violaceum</i>	0.0320	0.0461	0.0309	-	-	-	-

1 = rbcL, 2 = ITS, 3 = trnH-psbA, 4 = rbcL + ITS, 5 = rbcL + trnH-psbA, 6 = ITS + trnH-psbA, 7 = rbcL + ITS + trnH-psbA

n/c: only single sequence available; -: sequence available for single barcode only

interspecific genetic distance of corresponding species in most cases. For instance, intraspecific genetic distance with ITS in *A. heterophyllum* was observed 0.0140, however, interspecific distances of *A. heterophyllum* were higher with other species like *A. stapfianum* (0.0417), *A. japonicum*

(0.0370), *A. violaceum* (0.0455) and *A. napellus* (0.0496). Similarly, the intraspecific genetic distance in *A. japonicum* was found 0.0021; and interspecific genetic distances were higher with other species- *A. heterophyllum* (0.0370), *A.*

violaceum (0.0291), *A. napellus* (0.0198) and *A. stapfianum* (0.0089).

Similarity-based

The discrimination rate of individual barcode and their combinations was highly variable (Table S5). Among individual barcodes, *rbcL* showed the lowest resolution for species discrimination while ITS showed the highest resolution (Table S5). ITS alone and combined with other barcodes (ITS + *rbcL*, ITS + *trnH-psbA* and *rbcL* + ITS + *trnH-psbA*), successfully discriminate the *A. heterophyllum* from other species. However, for other four species (*A. violaceum*, *A. napellus*, *A. stapfianum* and *A. japonicum*) ITS showed low resolution and discriminated the sequences at the genus level only. Other barcodes like *rbcL* and *trnH-psbA* and their combination did not discriminate the sequences even at the genus level.

Comparison of species discriminations rate of three methods used

Among the three methods (NJ, PWG-Distance, and Blast) used to assess the effectiveness of species discrimination

for DNA barcodes and combinations, the PWG-distance method was found the best (Fig. 3A). The *rbcL* showed zero discrimination rate in all the three methods used, thus excluded from further comparisons. The discrimination rate of PWG- distance ranged from 33.3% (*rbcL*+*trnH-psbA*) to 100% (ITS, *rbcL*+ITS, ITS +*trnH-psbA* and *rbcL* + ITS + *trnH-psbA*). The NJ method was found second best to discriminate the *Aconitum* species with a discrimination rate of 20% (*trnH-psbA*) to 66.6% (*rbcL* + *trnH-psbA*), and BLAST was found least effective with a discrimination rate of 20% (*trnH-psbA*) to 40% (ITS).

Discrimination efficiency of individual barcode and their combination

With respect to recognition rates for single barcodes, the ITS marker had the highest degree of species discrimination (NJ-40%, PWG-100% and BLAST-40%), followed by *trnH-psbA* (NJ-20%, PWG-60% and BLAST-20%), but *rbcL* had the lowest level (0%) (Fig. 3A). The species resolution of the *rbcL* DNA region is less effective. Among combinations, both ITS + *trnH-psbA* and *rbcL* + ITS + *trnH-psbA* had the same level (NJ-33.3%, PWG-100% and BLAST-33.3%) of species discrimination.

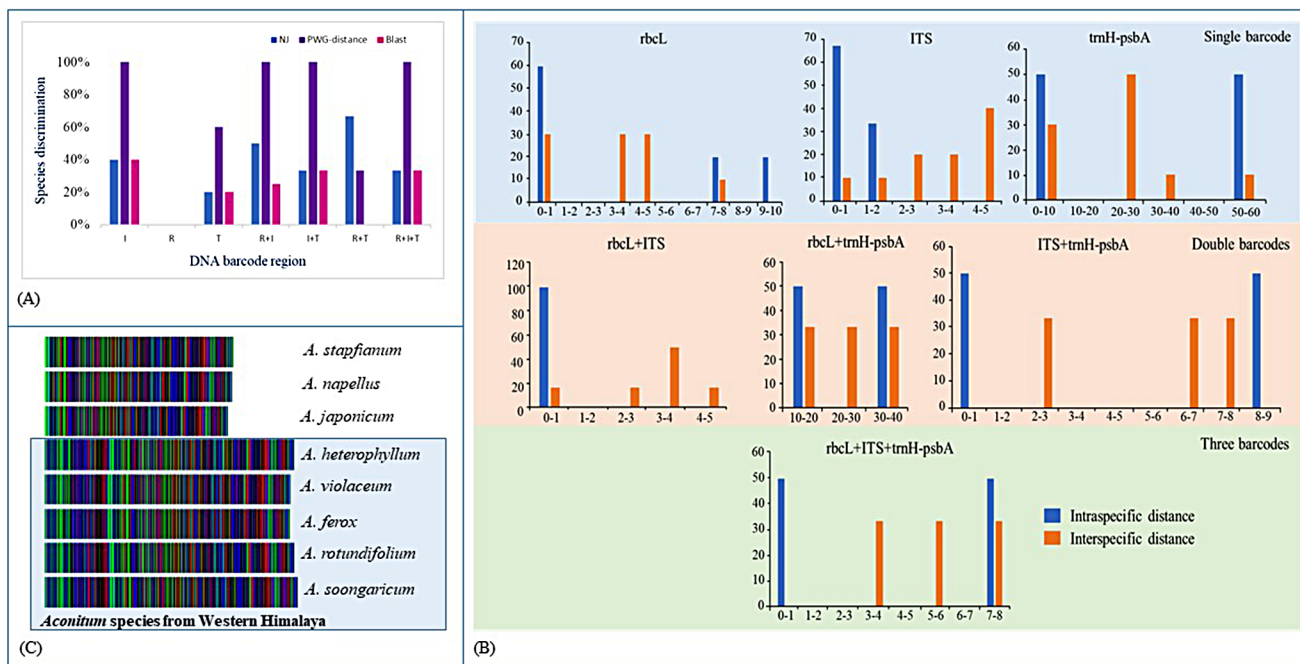


Fig. 3 DNA barcode analysis in *Aconitum* species. **(A)** Comparison of species discrimination success of single barcode region and their combinations based on NJ-tree, PWG-distance and BLAST method. I=ITS, R=*rbcL*, and T=*trnH-psbA*. Bar diagram suggested that PWG-distance approach is the best among three approaches used. However, among barcode genes, ITS found best for species discrimination. **(B)** Barcoding gap assessment for markers *rbcL*, ITS, *trnH-psbA* and their possible combinations in *Aconitum*. x-axes represent

K2P distance intervals and y-axes represent the percentage of occurrences. With the increase in K2P distance intervals. ITS performed best with higher barcode gap with interspecies distance as compared to the intraspecies distance **(C)** Linear DNA barcode of *Aconitum spp.* based on the ITS gene. The sequence length of the available ITS genes varies and this might be the possible reason for the length variation of developed barcodes

Assessment of DNA barcoding gap

For the assessment of barcoding gap, we calculated mean genetic distance within and between species under Kimura-2-parameter distance (Table 5) and plotted K2P distance against percentage occurrence of single marker and, their combination (Fig. 3B). The range of average genetic distance within/between various species of *Aconitum* with K2P were 0.0–9.31% / 0.0–7.44% for *rbcL*, 0.21–1.40% / 0.89–4.96% for ITS, 0.0–54.82% / 0.71–58.20% for *trnH-psbA*, 0.22–0.54% / 0.8–4.10% for *rbcL* + ITS, 0.0–21.89% / 4.49–16.42% for *rbcL* + *trnH-psbA*, 0.34–8.63% / 2.76–7.26% for ITS + *trnH-psbA* and 0.29–7.14% / 3.81–7.33% for *rbcL* + ITS + *trnH-psbA* (Table 5). The genetic distance method based on histograms exhibited overlap between intra- and interspecific distance. ITS had higher barcoding gap as compared to other individual barcodes and their combinations (Fig. 3B).

Discrimination of *Aconitum* species present in Western Himalaya

We also analyzed six *Aconitum* species (*A. balfourii*, *A. ferox*, *A. heterophyllum*, *A. rotundifolium*, *A. soongaricum* and *A. violaceum*) existing in Western Himalaya. For these species total 54 sequences for *rbcL* and ITS barcode regions retrieved from NCBI database is shown in Table S6. For the *trnH-psbA*, no sequences were available on NCBI database, thus did not include in the analysis. These species were distinguished clearly through tree-based method using the ITS barcode gene with 100% species resolution, while *rbcL* showed very poor species resolution (Fig. S2); and suggested the efficient performance of ITS over the *rbcL* for discrimination of *Aconitum* species of Western Himalaya.

Moreover, in case of ITS, intraspecific genetic distance was found lower than the interspecific genetic distance of corresponding species in most cases. For instance, intraspecific genetic distance in *A. ferox* was observed 0.0222, however, interspecific genetic distances of *A. ferox* with other species ranged 0.0379–0.0686. Likewise, intraspecific genetic distance in *A. heterophyllum* and *A. rotundifolium* were 0.0298 and 0 (zero) whereas interspecific genetic distances with other species ranged 0.0399–0.0686 and 0.0265–0.0399 respectively (Table S7). The minimum interspecific mean distance was observed in *A. rotundifolium* and *A. soongaricum* (0.0265) and the maximum in *A. ferox* and *A. heterophyllum* (0.0686).

Validation of species discrimination of ITS with larger dataset

To validate the species discrimination power of ITS, we used 643 sequences (including ITS sequences available on NCBI database and sequences generated during the present study) representing 64 *Aconitum* spp (Fig. S3). The *Aconitum* spp. with ≤ 3 ITS sequences were excluded from the analysis to reduce the confounding. Out of 64 *Aconitum* spp., 36 spp. were grouped into particular clades, including 13 *Aconitum* spp. where all the individuals come together. However, remaining 23 spp. were clubbed with other *Aconitum* spp. but in a single clade. For some *Aconitum* spp, the majority of sequences grouped together, but few sequences were grouped in different clades. For instance, all sequences the six *Aconitum* spp. like *A. anthoroideum*, *A. baicalense*, *A. contortum*, *A. ciliare*, *A. liangshanicum*, and *A. nemorum* were grouped together except for one sequence. Similarly, in the case of *A. lycoctonum*, out of 15 sequences, 12 were grouped together, however, the remaining 3 sequences were little dispersed and intermingled with other spp. but at a short distance.

Further, we also identified some species-specific sequence variation in ITS gene. For instance, in case of *A. coreanum*, three variations including deletion of 2 nucleotides, insertion of 2 nucleotides and one SNP (C/G) were identified at different positions. Similarly, in case of *A. bicalense* (one nucleotide deletion) and *A. gymnantrum* (three nucleotides deletion) species-specific mutations were observed. For *A. heterophyllum*, one SNP was observed where allele “A” is specifically present in *A. heterophyllum* while other *Aconitum* spp. contained allele “C or T”.

Barcode generation

Among all the DNA barcodes and their combinations, ITS showed the best species discrimination power and was used to develop species-specific barcodes for *Aconitum* species (Fig. 3C). Electronic devices can read information from DNA fragments and can be used to identify species.

Discussion

The *Aconitum* species, under the present study, are included in the IUCN Red List due to their exploitation for medicinal uses [19–21], with *A. heterophyllum* and *A. violaceum* categorized as ‘Endangered’ and ‘Vulnerable’ respectively [40]. The development of DNA barcodes is important in the case of *Aconitum* species because conventional methods mainly focus on floral characteristics for identifying plants. For instance, in *Aconitum* genus tuberous roots have medicinal

values, in that case, it is difficult to identify vegetative or fragmented plant samples [41]. Further, it is difficult to accurately identify the species growing in their native habitats in their vegetative state. Thus, DNA barcodes play a significant role in the identification of species. However, only limited efforts have been done for species discrimination in *Aconitum* and needs to be further explored. For instance, DNA barcode region psbA-trnH intergeneric spacer region found useful marker for the authentication of 19 taxa of *Aconitum* which are occurring in China [23]. However, none of them has any occurrence in the Himalayan region. It was suggested that psbA-trnH intergenic spacer analysis can distinguish most of the *Aconitum* medicinal species, but with limited differentiation power for the variants. In another study, rbcL locus showed the successful discrimination between *A. heterophyllum* and *A. balfourii* and thus suggested for the authentication of their traded parts like dried rhizomes obtained from market [26, 42] designed nrDNA ITS sequence-based SCAR (Sequence Characterized Amplified Region) markers to authenticate *Aconitum heterophyllum* (Ativisha) and *Cyperus rotundus* (Musta) at the raw drug source and in prepared herbal products. Further [43], developed a 23 bp genus-specific nucleotide signature which they found was unique to *Aconitum* species and is conserved within the genus and utilized this to differentiate 79 species which are occurring in China [44] undertook complete chloroplast (CP) genome sequencing of 10 species of *Aconitum* which was found to be beneficial in determining the complex phylogenetic relationships among these species. They also carried out data comparison with other sequenced species in GenBank database. For phylogenetic interference of *Aconitum* spp., two phylogenetic techniques, namely ITS (632 sequences from 164 spp.) and linked housekeeping proteins present in the chloroplast (rbcL and matK from 29 spp.), have recently been studied [45].

The goal of this work was to create an effective DNA marker that will enable individual DNA barcodes and their combinations to identify the two different species of *Aconitum* species from Western Himalaya, which are threatened in their native habitats. Different analytical techniques have been used to evaluate the ability to distinguish between species, including tree-based (NJ), distance-based (PWG-distance), and sequence similarity-based (BLAST) techniques on the same data set, each of these techniques had a different level of discrimination power. The present study demonstrated that sequence-based phylogenetic analysis and barcoding gap of ITS showed the best result to identify the *Aconitum* species. Amplification of matK showed a lower rate of sequence recovery [46].

A total of 45 sequences of rbcL, 39 sequences of ITS, and 8 sequences of trnH-psbA were utilized to construct phylogenetic trees (NJ). Because there were fewer trnH-psbA

sequences in the NCBI GenBank database, the number of sequences decreased in two and three gene combinations. *A. napellus* and *A. japonicum* were eliminated from further analysis because all the three region's sequences were not available for the same individual. As a result, the rbcL + ITS phylogenetic tree analysis includes four species, while the other combinations three species. In terms of species discrimination, ITS followed by rbcL + ITS provided a higher resolution and was more effective at identifying medicinal *Aconitum* species. ITS sequences of *A. heterophyllum* showed successful results at species level whereas *A. violaceum* at genus level because of the limited sequences of the *A. violaceum* ITS region in the NCBI GenBank database. The non-availability of sequences for *A. violaceum* and *A. stapfianum* in the NCBI GenBank database may be one of the explanations of genus level discrimination. The rbcL had 124 bases long sequences because of the trimming after alignment at both the ends (5' and 3') to get the best alignment.

ITS had 51 variable sites and only five (5) indel events which indicates the highest number of SNPs (Single Nucleotide Polymorphisms) among individual DNA barcodes. SNPs can cause variations in phenotypic characteristics among individuals of a species [47]. Thus, these SNPs might be a possible explanation in support of higher species discrimination through the ITS DNA barcode. trnH-psbA is highly variable DNA barcode of the plastid region [5, 48]. In present study, ITS had 450 bases long aligned sequences and 51 total mutations (Eta) whereas trnH-psbA 157 bases and 65 total mutations. These observations suggested that the number of mutations does not depend on sequence length.

A negative Tajima's D for all, markers except rbcL + ITS denotes an excess of low frequency polymorphisms in comparison to expectations (Table 4), which indicates population growth. A favourable low amount of both low and high frequencies of polymorphisms are indicated by positive Tajima's D value, which denotes a shrinking population. The negative Fu's Fs test statistic in ITS showed recent population growth. In Figure S1 expected values (green line) represent constant population size and observed values (red line) represent the deviation from it.

An optimal DNA barcoding sequence for species identification should demonstrate that genetic variation across species is significantly greater than the genetic variance within species. When performing a within-species mean distance analysis and a between-species mean distance analysis, we excluded species that had a single sequence and those that lacked distinct DNA barcode for the same species. All pairwise genetic distances were estimated for each individual species using MEGA X's application of the Kimura 2-parameter model (K2P%) [49]. Since DNA barcoding

studies typically employ this technique, we employed K2P%. The highest barcoding gap was found in ITS.

In the present study, PWG and NJ trees had greater identification rates compared to BLAST. This is also supported by other studies [50, 51]. The influence of redundant genes may have decreased BLAST's resolution. The best species resolution among all single candidate DNA barcodes in our research was found in ITS markers. The same outcome was shown in prior studies [46, 52, 53]. In the present study, rbcL + ITS, ITS + trnH-psbA, and rbcL + ITS + trnH-psbA showed increased discrimination power at species level as compared to single rbcL and trnH-psbA. This is the combined effect of ITS with another barcode region. High resolving ability of ITS, either alone in *Ficus* and *Gossypium* species [54], Palm [55] and some timber species (Meliaceae) [56] or in combination with rbcL and/or matK in *Lysimachia* [15] and Palm [55] was also reported. In our study rbcL was not able to show species discrimination using any of the methods used like NJ, PWG-distance and BLAST. The DNA barcode rbcL is frequently used in phylogenetic research and is very helpful at the family and genus levels with good universality across various taxa is one of the explanations [53]. The second explanation is the short length (124 bases) of aligned sequences. In the present study, *Aconitum* species are more closely related to each other within single genera. It is evident that rbcL is effective at genus-level discrimination, below the genus level their discrimination power decreases [53]. At the species level, the rbcL markers showed only 10% discriminating ability in *Alnus* [52] and 26% in *Arecaceae* [55]. In another study, rbcL showed lower (24.7–28.5%) species discrimination power among tropical trees from Xishuangbanna Nature Reserve in China [57]. In contrast, ITS DNA barcode which had maximum aligned sequence length (450 bases) among individual DNA barcodes showed the best level of species discrimination. Based on rbcL and ITS sequence length and discrimination rate we interpreted that it is best to use long aligned sequences for higher species discrimination rate.

After alignment of rbcL + ITS sequence, it showed 100% base composition similarity with ITS, however, there was variation in length. The only difference was rbcL + ITS had more gaps or missing sites as compared to ITS. In Fig. 3B, DNA barcode only contains nucleotide bases not gaps/missing sites, this is one of the explanations that both sequences are of the same length.

For the construction of phylogenetic tree of *Aconitum* species of Western Himalaya, total 45 sequences of rbcL and 9 sequences of ITS were used. The rbcL and ITS barcode sequences for *A. rotundifolium* and *A. balfourii*, respectively, were not available in the NCBI database. Similar to other *Aconitum* species (*A. heterophyllum*, *A. japonicum*, *A. napellus*, *A. stapfianum*, and *A. violaceum*), the ITS barcode

region was successful in differentiating between *Aconitum* species found in the Western Himalaya. In previous studies, the same result was demonstrated where ITS found the most efficient DNA barcode to discriminate plant species like *Alnus*, *Crawfordia*, *Hippaphae* etc. [46, 52, 53, 58]. The NJ tree and interspecific mean distance analysis suggested that *A. rotundifolium* and *A. soongaricum* are closer, while *A. ferox* and *A. heterophyllum* are less close as compared to other species of Western Himalaya.

Altogether, ITS found the best DNA barcode to discriminate the *Aconitum* spp., as it discriminates the majority of the *Aconitum* spp. (Fig S3). NJ tree of 643 sequences revealed the potential of ITS barcode, where most of the sequences were grouped in a species-specific manner. Although some sequences were clustered with non-specific clades. There might be two possible reasons for this discrepancy- (i) some technical error during sequencing etc. or (ii) wrong nomenclature of the spp. Similar observations were also highlighted and discussed in recent review [45]. Further, species-specific sequence variation is found to be very important in order to develop markers to distinguish a particular species. It becomes even more important if some species are commercially potential and others are toxic in nature. We also observed species-specific sequence variation in ITS gene. Maximum species-specific sequence variation was observed in *A. coreanum* with one insertion, one deletion and one SNP; suggested that *A. coreanum* is most evolved. Similar observation for *A. coreanum* has also been made while analysing the sequence variation ndhC-trnV region in earlier study [59].

In conclusion, The PWG-distance method was found most effective for species discrimination and ITS showed the best species discrimination power and was used to develop species-specific barcodes for *Aconitum* species. The DNA barcodes developed during the present study would be a potential tool for the identification of *Aconitum* species with particular emphasis on species of Western Himalaya.

Supplementary Information The online version contains supplementary material available at <https://doi.org/10.1007/s11033-023-08927-y>.

Acknowledgements This study was supported by the Council of Scientific and Industrial Research (CSIR) (MLP-172). AC thanks CSIR for the Junior Research Fellowship. This manuscript represents CSIR-IHBT communication number 5430.

Author contributions AC- data acquisition, wet-lab experiments, analysis, writing; DS- data acquisition; JP- data acquisition; KS and SS- plant sample collection; AC- conceptualization, plant material and sampling, editing; VJ-conceptualization, supervision, result interpretation, writing and editing.

Funding This study was funded by the Council of Scientific and Industrial Research (CSIR) (MLP-172).

Data Availability All data needed to support the conclusions are included in this article. Additional data related to this paper can be requested from the corresponding author.

Declarations

Conflict of interest The authors have no conflicts of interest to declare that are relevant to the content of this article.

Ethics approval and consent to participate This article does not contain any studies with human participants or animals performed by any of the authors.

References

- Rajphriyadharshini R, Weerasena OV (2020) DNA barcoding of medicinal plant: a systemic review. *Int J Pharm Sci Invent* 9:06–16. <https://doi.org/10.35629/6718-09060616>
- Badola HK, Aitken S (2003) The himalayas of India: a treasury of medicinal plants under siege. *Biodiversity* 4:3–13. <https://doi.org/10.1080/14888386.2003.9712694>
- Safhi FA, Alshamrani SM, Jalal AS, El-Moneim DA, Alyamani AA, Ibrahim AA (2022) Genetic characterization of some Saudi Arabia's accessions from *Commiphora gileadensis* using physio-biochemical parameters, molecular markers, DNA barcoding analysis and relative gene expression. *Genes* 13:2099. <https://doi.org/10.3390/genes13112099>
- Hebert PD, Cywinska A, Ball SL, DeWaard JR (2003) Biological identifications through DNA barcodes. *Proc R Soc B: Biol Sci* 270:313–321. <https://doi.org/10.1098/rspb.2002.2218>
- Kress WJ, Wurdack KJ, Zimmer EA, Weigt LA, Janzen DH (2005) Use of DNA barcodes to identify flowering plants. *Proc Natl Acad Sci* 102:8369–8374. <https://doi.org/10.1073/pnas.0503123102>
- Kress WJ (2017) Plant DNA barcodes: applications today and in the future. *J Syst Evol* 55:291–307. <https://doi.org/10.1111/jse.12254>
- Hollingsworth ML, Andra Clark AL, Forrest LL, Richardson J, Pennington RT, Long DG, Cowan R, Chase MW, Gaudeul M, Hollingsworth PM (2009) Selecting barcoding loci for plants: evaluation of seven candidate loci with species-level sampling in three divergent groups of land plants. *Mol Ecol Resour* 9:439–457. <https://doi.org/10.1111/j.1755-0998.2008.02439.x>
- Hollingsworth PM, Graham SW, Little DP (2011) Choosing and using a plant DNA barcode. *PLoS ONE* 6:e19254. <https://doi.org/10.1371/journal.pone.0019254>
- Fazekas AJ, Kesanakurti PR, Burgess KS, Percy DM, Graham SW, Barrett SC, Newmaster SG, Hajibabaei M, Husband BC (2009) Are plant species inherently harder to discriminate than animal species using DNA barcoding markers? *Mol Ecol Resour* 9:130–139. <https://doi.org/10.1111/j.1755-0998.2009.02652.x>
- Chase MW, Fay MF (2009) Barcoding of plants and fungi. *Science* 325:682–683. <https://doi.org/10.1126/science.1176906>
- Chen S, Yao H, Han J, Liu C, Song J, Shi L, Zhu Y, Ma X, Gao T, Pang X, Luo K, Li Y, Li X, Jia X, Lin Y, Leon C (2010) Validation of the ITS2 region as a novel DNA barcode for identifying medicinal plant species. *PLoS ONE* 5:e8613. <https://doi.org/10.1371/journal.pone.0008613>
- CBOL Plant Working Group 1, Hollingsworth PM, Forrest LL, Spouge JL, Hajibabaei M, Ratnasingham S, Bank MVD, Chase MW, Cowan RS, Erickson DL, Fazekas AJ, Graham SW, James KE, Kim KJ, Kress WJ, Schneider H, AlphenStahl JV, Barrett SCH, Berg CVD et al (2009) A DNA barcode for land plants. *Proc Natl Acad Sci* 106:12794–12797. <https://doi.org/10.1073/pnas.0905845106>
- Li FW, Kuo LY, Rothfels CJ, Ebihara A, Chiou WL, Windham MD, Pryer KM (2011) rbcL and matK earn two thumbs up as the core DNA barcode for ferns. *PLoS ONE* 6:e26597. <https://doi.org/10.1371/journal.pone.0026597>
- Xiang XG, Hu HA, Wang WE, Jin XH (2011) DNA barcoding of the recently evolved Genus *Holcoglossum* (Orchidaceae: Aeridinae): a test of DNA barcode candidates. *Mol Ecol Resour* 11:1012–1021. <https://doi.org/10.1111/j.1755-0998.2011.03044.x>
- Zhang CY, Wang FY, Yan HF, Hao G, Hu CM, Ge XJ (2012) Testing DNA barcoding in closely related groups of *Lysimachia* L. (Myrsinaceae). *Mol Ecol Resour* 12:98–108. <https://doi.org/10.1111/j.1755-0998.2011.03076.x>
- Li X, Yang Y, Henry RJ, Rossetto M, Wang Y, Chen S (2015) Plant DNA barcoding: from gene to genome. *Biol Rev* 90:157–166. <https://doi.org/10.1111/brv.12104>
- Safhi FA, Alshamrani SM, Bogmaza AF, El-Moneim DA (2023) DNA barcoding of wild plants with potential Medicinal properties from Faifa Mountains in Saudi Arabia. *Genes* 14:469. <https://doi.org/10.3390/genes14020469>
- Wood C, Coulson J, Thompson J, Bonner S (2020) An intentional aconite Overdose: a case report. *J Crit Care Med* 6:124–129. <https://doi.org/10.2478/jccm-2020-0016>
- Yun YE, Yu JN, Nam GH, Ryu SA, Kim S, Oh K, Lim CE (2015) Next-generation sequencing identification and characterization of microsatellite markers in *Aconitum austrokoreense* Koidz., an endemic and endangered medicinal plant of Korea. *Genet Mol Res* 14:4812–4817. <https://doi.org/10.4238/2015.May.11.13>
- Kong H, Liu W, Yao G, Gong W (2018) Characterization of the whole chloroplast genome of a rare and endangered species *Aconitum reclinatum* (Ranunculaceae) in the United States. *Conserv Genet Resour* 10:165–168. <https://doi.org/10.1007/s12686-017-0789-y>
- Wani TA, Kaloo ZA, Dangroo NA (2022) *Aconitum heterophyllum* Wall. Ex Royle: a critically endangered medicinal herb with rich potential for use in medicine. *J Integr Med* 20:104–113. <https://doi.org/10.1016/j.joim.2021.12.004>
- Kumar A, Tiwari A, Narendran P, Raturi PP (2023) Genetic diversity and population structure of *Aconitum heterophyllum*-an endangered plant from North-Western Himalayas using microsatellite markers. *Med Plants Int J* 15:390–401. <https://doi.org/10.5958/0975-6892.2023.00039.4>
- He J, Wong KL, Shaw PC, Wang H, Li DZ (2010) Identification of the medicinal plants in *Aconitum* L. by DNA barcoding technique. *Planta Med* 76:1622–1628. <https://doi.org/10.1055/s-0029-1240967>
- Ren YY (2018) Identification of tibetan medicinal plants of *Aconitum* Genus by ITS2 sequences. *Chin Tradit Herb Drugs* 24:4614–4620
- Almerekova S, Ivaschenko A, Kaparbay R, Myrzagalieva A, Turuspekov Y (2020) Phylogenetic assessment of tree species of *Aconitum* L. from Kazakhstan by using ITS and matK markers. *Eurasian Union of Scientists* 2:4–9. <https://doi.org/10.31618/ESU.2413-9335.2020.2.79.1036>
- Negi RK, Nautiyal P, Bhatia R, Verma R (2021) rbcL, a potential candidate DNA barcode loci for aconites: conservation of himalayan aconites. *Mol Biol Rep* 48:6769–6777. <https://doi.org/10.1007/s11033-021-06675-5>
- Sharma P, Samant SS, Lal M, Sharma A (2014) Diversity, indigenous uses, threat categorization and conservation prioritization of medicinal plants: a case study from Himachal Pradesh, India. *J Biodivers Endanger Species* 2:2. <https://doi.org/10.4172/2332-2543.1000134>
- Thakur KS, Kumar M, Bawa R, Busmann RW (2014) Ethnobotanical study of herbaceous flora along an altitudinal gradient in

- Bharmour Forest Division, District Chamba of Himachal Pradesh, India. <https://doi.org/10.1155/2014/946870>. J Evid Based Complementary Altern Med
29. Jishtu V, Bhondge SW, Bhushan B, Chauhan M, Chauhan A (2021) Threatened ethnomedicinal plants of Dodra-Kwar region of Himachal Pradesh, NW Himalaya. J Med Plants Stud 9:151–159
 30. Doyle JJ, Doyle JL (1987) A rapid DNA isolation procedure for small quantities of fresh leaf tissue. Phytochem Bull 19:11–15
 31. Kumar S, Stecher G, Li M, Knyaz C, Tamura K (2018) MEGA X: molecular evolutionary genetics analysis across computing platforms. Mol Biol Evol 35:1547–1549. <https://doi.org/10.1093/molbev/msy096>
 32. Rozas J, Ferrer-Mata A, Sánchez-DelBarrio JC, Guirao-Rico S, Librado P, Ramos-Onsins SE, Sánchez-Gracia A (2017) DnaSP 6: DNA sequence polymorphism analysis of large data sets. Mol Biol Evol 34:3299–3302. <https://doi.org/10.1093/molbev/msx248>
 33. Tajima F (1989) Statistical method for testing the Neutral mutation hypothesis by DNA polymorphism. Genetics 123:585–595. <https://doi.org/10.1093/genetics/123.3.585>
 34. Fu YX (1997) Statistical tests of neutrality of mutations against population growth, hitchhiking and background selection. Genetics 147:915–925. <https://doi.org/10.1093/genetics/147.2.915>
 35. Srivathsan A, Meier R (2012) On the inappropriate use of Kimura-2-parameter (K2P) divergences in the DNA-barcoding literature. Cladistics 28:190–194. <https://doi.org/10.1111/j.1096-0031.2011.00370.x>
 36. Collins RA, Cruickshank RH (2013) The seven deadly sins of DNA barcoding. Mol Ecol Resour 13:969–975. <https://doi.org/10.1111/1755-0998.12046>
 37. Yan LJ, Liu J, Möller M, Zhang X, Li DZ, Gao LM (2015) DNA barcoding of *Rhododendron* (Ericaceae), the largest Chinese plant genus in biodiversity hotspots of the Himalaya–Hengduan Mountains. Mol Ecol Resour 15:932–944. <https://doi.org/10.1111/1755-0998.12353>
 38. Kress WJ, Erickson DL (2007) A two-locus global DNA barcode for land plants: the coding rbcL gene complements the non-coding trnH-psbA spacer region. PLoS ONE 2:e508. <https://doi.org/10.1371/journal.pone.0000508>
 39. Krawczyk K, Szczecińska M, Sawicki J (2014) Evaluation of 11 single-locus and seven multilocus DNA barcodes in *Lamium* L. (Lamiaceae). Mol Ecol Resour 14:272–285. <https://doi.org/10.1111/1755-0998.12175>
 40. Jabeen N, Kozgar M, Dar GH, Shawl AS, Khan S (2013) Distribution and taxonomy of genus *Aconitum* in Kashmir: potent medicinal resource of Himalayan Valley. Chiang Mai J Sci 40:173–186
 41. Shyaula SL (2011) Phytochemicals, traditional uses and processing of *Aconitum* species in Nepal. Nepal J Sci Technol 12:171–178
 42. Seethapathy GS, Balasubramani SP, Venkatasubramanian P (2014) nrDNA ITS sequence-based SCAR marker to authenticate *Aconitum heterophyllum* and *Cyperus rotundus* in Ayurvedic raw drug source and prepared herbal products. Food Chem 145:1015–1020. <https://doi.org/10.1016/j.foodchem.2013.09.027>
 43. Wang G, Liu Y, Bai X, Cao P, Pang X, Han J (2022) Identification and Poisoning diagnosis of *Aconitum* materials using a genus-specific nucleotide signature. Ecotoxicol Environ Saf 237:113539. <https://doi.org/10.1016/j.ecoenv.2022.113539>
 44. Xia C, Wang M, Guan Y, Li J (2022) Comparative analysis of the chloroplast genome for *Aconitum* species: genome structure and phylogenetic relationships. Front Genet 13:878182. <https://doi.org/10.3389/fgene.2022.878182>
 45. Kakkar RA, Haneen MA, Parida AC, Sharma G (2023) The known, unknown, and the intriguing about members of a critically endangered traditional medicinal plant genus *Aconitum*. Front Plant Sci 14:1139215. <https://doi.org/10.3389/fpls.2023.1139215>
 46. Zhang D, Jiang B, Duan L, Zhou N (2016) Internal transcribed spacer (ITS), an ideal DNA barcode for species discrimination in *Crawfordia* Wall. (Gentianaceae). Afr J Tradit Complement Altern Med 13:101–106. <https://doi.org/10.21010/ajteam.v13i6.15>
 47. Huq MA, Akter S, Nou IS, Kim HT, Jung YJ, Kang KK (2016) Identification of functional SNPs in genes and their effects on plant phenotypes. J Plant Biotechnol 43:1–11. <https://doi.org/10.5010/JPB.2016.43.1.1>
 48. Shaw J, Lickey EB, Schilling EE, Small RL (2007) Comparison of whole chloroplast genome sequences to choose noncoding regions for phylogenetic studies in angiosperms: the tortoise and the hare III. Am J Bot 94:275–288. <https://doi.org/10.3732/ajb.94.3.275>
 49. Kimura M (1980) A simple method for estimating evolutionary rates of base substitutions through comparative studies of nucleotide sequences. J Mol Evol 16:111–120. <https://doi.org/10.1007/BF01731581>
 50. Xie L, Wang YW, Guan SY, Xie LJ, Long X, Sun CY (2014) Prospects and problems for identification of poisonous plants in China using DNA barcodes. Biomed Environ Sci 27:794–806. <https://doi.org/10.3967/bes2014.115>
 51. Wang J, Zhao J, Yu W, Wang S, Bu S, Shi X, Zhang X (2021) Rapid identification of common poisonous plants in China using DNA barcodes. Front Ecol Evol 9:698418. <https://doi.org/10.3389/fevo.2021.698418>
 52. Ren BQ, Xiang XG, Chen ZD (2010) Species identification of *Alnus* (Betulaceae) using nrDNA and cpDNA genetic markers. Mol Ecol Resour 10:594–605. <https://doi.org/10.1111/j.1755-0998.2009.02815.x>
 53. China Plant BOL Group 1, Li DZ, Gao LM, Li HT, Wang H, Ge XJ, Liu JQ, Chen ZD, Zhou SL, Chen SL, Yang JB, Fu CX, Zeng CX, Yan HF, Zhu YJ, Sun YS, Chen SY, Zhao L, Wang K et al (2011) Comparative analysis of a large dataset indicates that internal transcribed spacer (ITS) should be incorporated into the core barcode for seed plants. Proc Natl Acad Sci 108:19641–19646. <https://doi.org/10.1073/pnas.1104551108>
 54. Roy S, Tyagi A, Shukla V, Kumar A, Singh UM, Chaudhary LB, Datt B, Bag Sk, Singh PK, Nair NK, Husain T, Tuli R (2010) Universal plant DNA barcode loci may not work in complex groups: a case study with Indian Berberis species. PLoS ONE 5:e13674. <https://doi.org/10.1371/journal.pone.0013674>
 55. Jeanson ML, Labat JN, Little DP (2011) DNA barcoding: a new tool for palm taxonomists? Ann Bot 108:1445–1451. <https://doi.org/10.1093/aob/mcr158>
 56. Muellner AN, Schaefer H, Lahaye R (2011) Evaluation of candidate DNA barcoding loci for economically important timber species of the mahogany family (Meliaceae). Mol Ecol Resour 11:450–460. <https://doi.org/10.1111/j.1755-0998.2011.02984.x>
 57. Huang XC, Ci XQ, Conran JG, Li J (2015) Application of DNA barcodes in Asian tropical trees—a case study from Xishuangbanna Nature Reserve, Southwest China. PLoS ONE 10:e0129295. <https://doi.org/10.1371/journal.pone.0129295>
 58. Liu ZF, Ci XQ, Li L, Li HW, Conran JG, Li J (2017) DNA barcoding evaluation and implications for phylogenetic relationships in Lauraceae from China. PLoS ONE 12:e0175788. <https://doi.org/10.1371/journal.pone.0175788>
 59. Park I, Kim WJ, Yang S, Yeo SM, Li H, Moon BC (2017) The complete chloroplast genome sequence of *Aconitum coreanum* and *Aconitum carmichaelii* and comparative analysis with other *Aconitum* species. PLoS One 12:e0184257. <https://doi.org/10.1371/journal.pone.0184257>

Publisher's Note Springer Nature remains neutral with regard to jurisdictional claims in published maps and institutional affiliations.

Springer Nature or its licensor (e.g. a society or other partner) holds exclusive rights to this article under a publishing agreement with the author(s) or other rightsholder(s); author self-archiving of the accepted manuscript version of this article is solely governed by the terms of such publishing agreement and applicable law.